
Article:
Curry, E. orcid.org/0000-0002-5123-8866, Muir, G., Qu, J. et al. (3 more authors) (2024) Engineering an Escherichia coli based in vivo mRNA manufacturing platform. Biotechnology and Bioengineering, 121 (6). pp. 1912-1926. ISSN 0006-3592

https://doi.org/10.1002/bit.28684

Received: 3 November 2023 | Revised: 31 January 2024 | Accepted: 15 February 2024

DOI: 10.1002/bit.28684

ARTICLE

BIOTECHNOLOGY AND BIOENGINEERING WILEY

Engineering an *Escherichia coli* based in vivo mRNA manufacturing platform

Edward Curry[1] | George Muir[1] | Jixin Qu[1] | Zoltán Kis[1] | Martyn Hulley[2] | Adam Brown[1]

[1]Department of Chemical and Biological Engineering, University of Sheffield, Sheffield, UK

[2]Bioprocess Development, AstraZeneca, Cambridge, UK

Correspondence

Adam Brown and Edward Curry, Department of Chemical and Biological Engineering, University of Sheffield, Mappin St., Sheffield S1 3JD, UK.
Email: adam.brown@sheffield.ac.uk and eajcurry1@sheffield.ac.uk

Funding information

Biotechnology and Biological Sciences Research Council; AstraZeneca, Grant/Award Number: BB/T508664/1

Abstract

Synthetic mRNA is currently produced in standardized in vitro transcription systems. However, this one-size-fits-all approach has associated drawbacks in supply chain shortages, high reagent costs, complex product-related impurity profiles, and limited design options for molecule-specific optimization of product yield and quality. Herein, we describe for the first time development of an in vivo mRNA manufacturing platform, utilizing an *Escherichia coli* cell chassis. Coordinated mRNA, DNA, cell and media engineering, primarily focussed on disrupting interactions between synthetic mRNA molecules and host cell RNA degradation machinery, increased product yields >40-fold compared to standard "unengineered" *E. coli* expression systems. Mechanistic dissection of cell factory performance showed that product mRNA accumulation levels approached theoretical limits, accounting for ~30% of intracellular total RNA mass, and that this was achieved via host-cell's reallocating biosynthetic capacity away from endogenous RNA and cell biomass generation activities. We demonstrate that varying sized functional mRNA molecules can be produced in this system and subsequently purified. Accordingly, this study introduces a new mRNA production technology, expanding the solution space available for mRNA manufacturing.

KEYWORDS

biopharmaceutical engineering, *E. coli*, mRNA manufacture, synthetic biology, synthetic mRNA

1 | INTRODUCTION

Synthetic mRNA has potential use in a wide range of applications, including cancer immunotherapy, protein replacement therapy, genome editing, pluripotent stem cell generation, and vaccines against infectious diseases (Baden et al., 2021; Breda et al., 2023; Gan et al., 2019; Qin et al., 2022; Vavilis et al., 2023). In all cases, mRNA molecules are currently produced in standardized in vitro transcription (IVT) systems, comprising an RNA Polymerase biocatalyst, DNA template, modified nucleosides, magnesium-containing buffer, and a capping enzyme/analog (Ouranidis et al., 2022). These simple, modular, cell-free production platforms embed flexibility and predictability in mRNA manufacture, while substantially reducing process-related impurities (Whitley et al., 2022). However, the requirement for purified input components is associated with relatively high costs, and critical reagent shortages (Kis et al., 2021).

Moreover, downstream purification processes are complicated by complex product-related impurity profiles, that include immunostimulatory double-stranded RNA and abortive transcripts (Gholamalipour et al., 2018; Rosa et al., 2021). However, despite these drawbacks, expanding product diversification (particularly with respect to size), highly variable intended applications (with associated variability in required production scale, purity, cost, etc.), and the increasing pressure placed on reagent/equipment supplies by growing demand for mRNA synthesis, there are currently no alternative technology platforms available for mRNA manufacture.

Cell-based production systems are the dominant choice for manufacture of other bioproducts, such as AAV vectors, recombinant proteins and recombinant DNA plasmids (Agostinetto et al., 2022; Jiang & Dalby, 2023; McElwain et al., 2022). Although they are associated with relatively complex and costly downstream processing steps to remove host-cell impurities, this is somewhat mitigated by the availability of well-characterized chromatographic and membrane-based unit operations (Fan et al., 2023; Sripada et al., 2022). As a relatively simple macromolecule, synthetic mRNA could theoretically be produced in virtually any microbial cell factory. *Escherichia coli* is a particularly attractive expression host given that decades of use in recombinant plasmid DNA production has led to development of very low-cost, standardized, easy to scale (up to 100,000 L) flexible manufacturing platforms (Pontrelli et al., 2018; Yang et al., 2021). Indeed, these benefits have seen *E. coli* utilized as a biocatalyst for production of RNA aptamers and double stranded RNA (dsRNA) molecules (Delgado-Martín & Velasco, 2021; Ma et al., 2020; Ponchon & Dardel, 2011; Ponchon et al., 2009, 2013).

The primary limitation of mRNA production in microbial expression hosts is endogenous pathways that encode rapid RNA turnover, where the average mRNA half-life in *E. coli* is ~5 min (Esquerré et al., 2015; Mohanty & Kushner, 2022). For dsRNA manufacture, multigram per liter yields have been achieved in *E. coli* bioprocesses by deleting RNase III, a nonessential dsRNA-targeting endonuclease (Pertzev, 2006). However, single stranded mRNA decay is mediated by RNAseE, an essential enzyme required for global RNA metabolism. Although RNAseE has broad substrate specificity, various sequence features have been shown to increase its relative specific activity on individual mRNA species, including unstructured AU rich regions, and, most critically, the presence of a 5′-monophosphate (Bae et al., 2023; Callaghan et al., 2005; Richards & Belasco, 2023). However, other molecule-specific features, such as RNA-binding protein binding sites, codon usage, and secondary structure profiles can reduce RNAse E mediated turnover of endogenous mRNA (Börner et al., 2023; Roux et al., 2022). For protein production in *E. coli*, recombinant mRNA stability is commonly enhanced by using bacterial 5′ untranslated regions (UTRs) containing secondary structures that prevent RNAse binding (Viegas et al., 2018), however, these elements are incompatible with manufacture of synthetic mRNA for mammalian cell applications. More generically, global mRNA half-life is affected by both the relative abundance and activity level of RNAse E (Mohanty & Kushner, 2022). Accordingly, the half-life of a specific mRNA molecule within an *E. coli* cell chassis is determined by a complex interplay between the mRNA sequence feature composition (e.g., codon adaptation index, GC content, presence of hairpin loops [Esquerré et al., 2015; Viegas et al., 2018]) and the host cell's complement of RNA degradation machinery components (e.g., RNAse E expression level [Mohanty & Kushner, 2022]).

Herein, we report coordinated mRNA, DNA, media and host cell engineering to dramatically increase synthetic mRNA accumulation and maintenance in *E. coli* cell factories. Achieving mRNA yields >40-fold greater than standard "unengineered" *E. coli* expression systems, we demonstrate rapid production and purification of a range of functional mRNA products. In doing so, we introduce a new technology platform for mRNA manufacturing solution spaces. This may be particularly useful in contexts where IVT systems are unavailable (e.g., due to reagent shortages), product formats necessitate process optimization (e.g., production of very large RNA molecules), or manufacturing costs need to be significantly reduced.

2 | MATERIALS AND METHODS

2.1 | Plasmid design and construction

The baseline mRNA production construct was designed with 5′ and 3′ UTR sequences from Xenopus beta-globin, directly flanking a human codon optimized eGFP sequence. All DNA sequences containing stabilization features of interest flanking the UTRs and coding sequence were synthesized and cloned into pET-24b (Novagen) by Twist Bioscience. Sequences were inserted using the BamHI and XhoI restriction sites, placing the GOI downstream of the T7 promoter and lac operon, and removing the ribosome binding site from the original plasmid. High copy number plasmids were constructed by amplifying the mRNA encoding region from the original pET29b (Novagen) vector by polymerase chain reaction (PCR), and inserting it into pRNA128A (Williams et al., 2010), a vector with the ColE1 origin of replication. Primer sequences can be found in Supporting Information: Table S2. Synthetic triple terminator constructs were assembled using DNA fragments purchased from Genewiz. The fragments consisted of the T3 and *E. coli* endogenous rrnB T1 terminators, and were ligated into vectors using the XhoI and BlpI restriction sites, directly upstream of the T7 terminator. Sequences of all DNA parts are available in Supporting Information: Table S1.

2.2 | Synthetic mRNA expression

mRNA encoding plasmids were transformed into BL21 (DE3) (F^-*ompT* *hsdS*$_B$ (r_B^-, m_B^-) *gal dcm* (DE3)) or BL21 Star (DE3) (F^-*ompT* *hsd*SB (r_B−, m_B−) *gal dcm rne*131 (DE3)) (Invitrogen) *E. coli* strains, typically used for recombinant protein production. Five milliliters of starter cultures were inoculated with a single colony, and grown overnight in Luria-Bertani (LB) broth (Thermo Fisher), containing 50 μg/mL

kanamycin (Thermo Fisher) at 37°C, 200 rpm. For small scale expression, 100 µL of starter culture was used to inoculate 10 mL of LB medium containing 50 µg/mL kanamycin, and cells were grown at 37°C, 200 rpm, until the $OD_{600\,nm}$ reached 0.4–0.6. For large scale expression, 200 mL of LB was inoculated with 5 mL of overnight culture. IPTG was then added to a final concentration of 1 mM. Where RNase E inhibitor was used (3-(4-Hydroxy-5-isopropyl-6-oxo-1,6-dihydro-pyrimidin-2-ylsulfanyl)-propionic acid [Santa Cruz Biotechnology], it was added from a 100× stock at the point of IPTG addition 500 µL of culture was pelleted at 30 min intervals postinduction, and pellets stored at −80°C. Cell concentrations were determined by taking the $OD_{600\,nm}$ of the culture through UV spectrophotometry, and applying the formula OD_{600} of 1.0 = 8×10^8 cells/mL. Total cellular capacity (integral of viable cell concentration), cell-specific growth rate, and cell-specific productivity were calculated as previously described (Brown et al., 2019).

2.3 | Commercial kit-based RNA extraction

Total RNA was extracted using the GenElute Total RNA purification kit (Sigma-Aldrich) according to the manufacturer's instructions. Briefly, cell pellets were resuspended in 100 µL of TE buffer containing 1 mg/mL Lysozyme, and incubated at room temperature for 5 min. Three hundred microliters of buffer RL and 200 µL of 96%–100% ethanol were added to the lysate before vortexing. Lysate was then applied to the spin column resin, before washing with ethanol solution. RNA was eluted in 50 µL of elution solution. Residual DNA in the RNA sample was then removed through addition of two units of RNase free DNase I, and incubation at 37°C for 30 min. RNA was purified from the DNase reaction using the Monarch RNA Cleanup kit (50 µg) (New England Biolabs), following the manufacturer's instructions. Briefly, two volumes of RNA binding buffer and three volumes of 96%–100% ethanol were added to the RNA sample. The RNA was then bound to the spin column resin, before washing with ethanol solution. RNA was eluted from the column in nuclease free water, and stored at −80°C. The concentration of samples was determined using a Nanodrop spectrophotometer (Thermo Fisher). Integrity of RNA samples were assessed using denaturing agarose gel electrophoresis. An equal volume of 2X RNA loading dye was added to 200 ng of total RNA, before heating to 65°C for 5 min, and loading on a 1% agarose gel, which was run at 80 V for 40 min.

2.4 | RNASwift-based RNA extraction

Two hundred microliters of *E. coli* culture was pelleted at 10,000×*g* for 10 min, before extraction by a protocol based upon RNASwift (Nwokeoji et al., 2016). Cells were suspended in 5 mL of 5 mg/mL lysozyme solution (Thermo Fisher), and allowed to lyse for 10 min at room temperature. Twelve milliliters of lysis solution (4% SDS, 0.5 M NaCl [Thermo Fisher]) was added, before incubation for 5 min at 65°C. 6.8 mL of 5 M NaCl of was added, and suspensions were placed on ice for 5 min to promote precipitation of SDS. Suspensions were centrifuged at 10,000×*g* for 20 min at 4°C, and supernatant was transferred to a separate tube. RNA was precipitated from the supernatant by isopropanol or ethanol, and stored at −20°C.

2.5 | Digital droplet PCR

Absolute product mRNA copy numbers were determined by one-step reverse transcription digital droplet PCR (RT-ddPCR). Primers were designed to amplify a 150 bp region in the middle of eGFP, universal to every construct under investigation. ddPCR reaction mixtures of a final volume of 20 µL were comprised of 5 µL one step RT-ddPCR supermix (Bio-Rad), 2 µL reverse transcriptase (Bio-Rad), 1 µL 300 mM DTT (Bio-Rad), 1 µL 900 nM forward/reverse primer mix (Integrated DNA Technologies), 1 µL 250 nM 5′-FAM probe (Integrated DNA Technologies), 9 µL H20 and 1 µL total RNA at a concentration of 1 ng/µL. The 20 µL reaction mixture and 70 µL of droplet generation oil (Bio-Rad) were loaded into a DG8 Cartridge, and 40 µL of droplets were generated with the Bio-Rad QX200 droplet generator. Droplets were transferred to a 96-well PCR plate (Bio-Rad), sealed with foil, and placed in a Bio-rad C1000 thermal cycler. Reverse transcription was performed at 50°C for 1 h. Polymerase activation was carried out for 10 min at 95°C, before 40 cycles of denaturation for 1 min at 95°C, before a combined annealing and extension phase for 1 min at 60°C. Enzymes were then deactivated at 98°C for 10 min, before a final hold phase at 12°C for 30 min. Positive droplets were detected by the QX200 droplet reader (Bio-Rad), using automatically assigned amplitude thresholds determined by QuantaSoft software (Bio-Rad). Samples were only used in analysis if the number of measured droplets exceeded 12,000.

2.6 | Magnetic bead-based mRNA purification

mRNA was purified from total RNA extraction samples by oligo-(dT) enrichment, using the Dynabeads mRNA purification kit (Invitrogen). Approximately 30 µg of total RNA was adjusted to a volume of 100 µL with nuclease free water. Samples were heated to 65°C for 2 min to disrupt secondary structure, before placing on ice. Magnetic beads were equilibrated in 100 µL of binding buffer (10 mM Tris-HCl, 1 M LiCl), before addition of the 100 µL total RNA samples. Beads were incubated with RNA samples for 5 min at room temperature with constant rotation, before removal of the supernatant. Beads were washed twice with 200 µL of washing buffer (10 mM Tris-HCl, 1 M LiCl). mRNA was eluted from the magnetic beads by addition of 10 mM Tris-HCl, pH 7.5, and its concentration determined by Nanodrop spectrophotometer.

2.7 | Liquid chromatography-based mRNA purification

mRNA from RNASwift-based extractions was purified by oligo-dT enrichment utilizing an ÄKTA pcc chromatography system (Cytiva). Ten milliliters of total RNA was bound to a 1 mL volume Oligo-dt(18) column (Sartorius) in binding buffer (50 mM Sodium Phosphate pH 7, 500 mM NaCl). The column was washed in 20 column volumes of wash buffer (50 mM sodium phosphate, 150 mM NaCl). Bound mRNA was eluted in 5 mL of water, before quantification by Nanodrop spectrophotometer.

2.8 | Capillary gel electrophoresis (CGE)

CGE analysis of RNA integrity and purity was performed with a 5200 Fragment Analyzer System (Agilent), using the DNF-471 RNA Kit (15 nt) (Agilent). The capillary cassette used was FA 12-Capillary Array Short, 33 cm (Agilent). Samples were diluted to <100 ng/µL in nuclease free water. Before each separation, a pre-run voltage was applied (8 kV for 30 s), the capillaries were conditioned with the conditioning solution and the capillaries were dipped twice in the rinse buffer. Following this, the capillaries were filled with RNA separation gel (by pressure) and then the sample was introduced using a voltage injection (5 kV for 4 s). The separation was then conducted by applying a voltage of 8 kV for 45 min. Detection was carried out using laser induced fluorescence, by fluorescent dye tagging of the RNA.

2.9 | Transfection of mRNA into HEK293 cells

Suspension adapted HEK293 cells (Thermo Fisher) were routinely cultured in serum-free medium (Thermo Fisher). Cells were maintained in 30 mL volume in 125 mL Erlenmeyer flasks (Corning), at 37°C, 85% humidity, and 5% CO_2, with agitation at 140 rpm. Cell density and viability was determined by the Countess 3 automated cell counter system (Thermo Fisher). mRNA that required capping before transfection was capped using the NEB Vaccinia virus capping system (New England Biolabs), following the manufacturers protocol cells for transfection were cultured in 24-shallow well plates (Corning), containing 500 µL culture volume, with agitation at 240 rpm. For mRNA transfection, cells were seeded at a density of 0.3×10^6 cells/mL in 24-shallow well plates, and incubated for 24 h. *Trans*IT-mRNA transfection reagent (Mirus) was used to transfect 500 ng of mRNA per well as per manufacturer's instructions. GFP transfection efficiency was determined by the Countess 3 system using a GFP filter. For fluorescence measurements, cells were by centrifugation at 200×*g* for 5 min, before resuspension in DPBS (Sigma-Aldrich), and determination of fluorescence by plate reader at 488 nm/507 nm.

3 | RESULTS AND DISCUSSION

3.1 | mRNA engineering to increase product stability in *E. coli*

The specific activity of RNAse E on a discrete mRNA species directly determines the half-life of that molecule in an *E. coli* cell chassis (Mauger et al., 2019; Mohanty & Kushner, 2022; Viegas et al., 2018). While coding sequence design could theoretically be employed to enhance accumulation of a particular mRNA molecule in *E. coli* (E.g., by optimizing codon-usage), the efficacy of such methods would be highly product-specific, dependent on the available design-space for each primary amino acid sequence. Algorithms are available for enhancing mRNA sequence through codon usage, however, the design rules applied are unlikely to produce sequences optimal for stability in both an *E. coli* and mammalian context (Leppek et al., 2022; Zhang et al., 2023). Accordingly, to achieve product-agnostic increases in mRNA stability, we focussed on engineering elements that are located outside the protein coding sequence. First, we introduced "scaffold" tRNA-Lysine motifs at both the 5′ and 3′ termini (TermtRNA-mRNA, Figure 1a), based on previous findings that (i) stable secondary structures significantly reduced the activity of RNAse E on mRNA molecules (Richards & Belasco, 2023; Zhang et al., 2021), and (ii) incorporation of tRNA motifs increased production of short RNA species in *E. coli* (Nelissen et al., 2012; Ponchon et al., 2009). As tRNA sequences from highly stable secondary and tertiary intramolecular interactions their presence at molecule termini should render mRNA products inaccessible to exonucleases and reduce the efficiency of RNAse binding at the 5′ monophosphate (Prossliner et al., 2023). Second, given that RNaseE is preferentially active on RNA species that have a 5′ monophosphate (Callaghan et al., 2005), we incorporated ribozyme sequences either side of the UTRs to promote self-circularization of product mRNA (SelfCirc-mRNA, Figure 1b). This design step was aided by recent work describing elements which efficiently catalyze mRNA self-circulation via the "Permuted Intron Exon" method (Rostain et al., 2020; Wesselhoeft et al., 2018). Lacking 5′ monophosphates and accessible termini these circularized molecules are resistant to exonucleases, and significantly protected from RNAseE mediated degradation (Richards & Belasco, 2016). Finally, we designed a hybrid approach, where sections of the tRNA-Lys motif were inserted at the 5′ and 3′ termini. Hybridization of these complementary sequences creates a pseudo-circular molecule, where the gene expression cassette is contained in a single stranded loop attached to the tRNA-Lys structural element (CirctRNA-mRNA, Figure 1c).

TermtRNA-, SelfCirc-, and CirctRNA-features were incorporated into the widely used protein expression vector pET29b, where transcription of product GFP mRNA was driven by the wild-type inducible T7 RNA polymerase promoter. These expression plasmids lacked a bacterial ribosome binding site (i.e., to prevent translation of GFP-mRNA in the host-cell) but contained commonly used

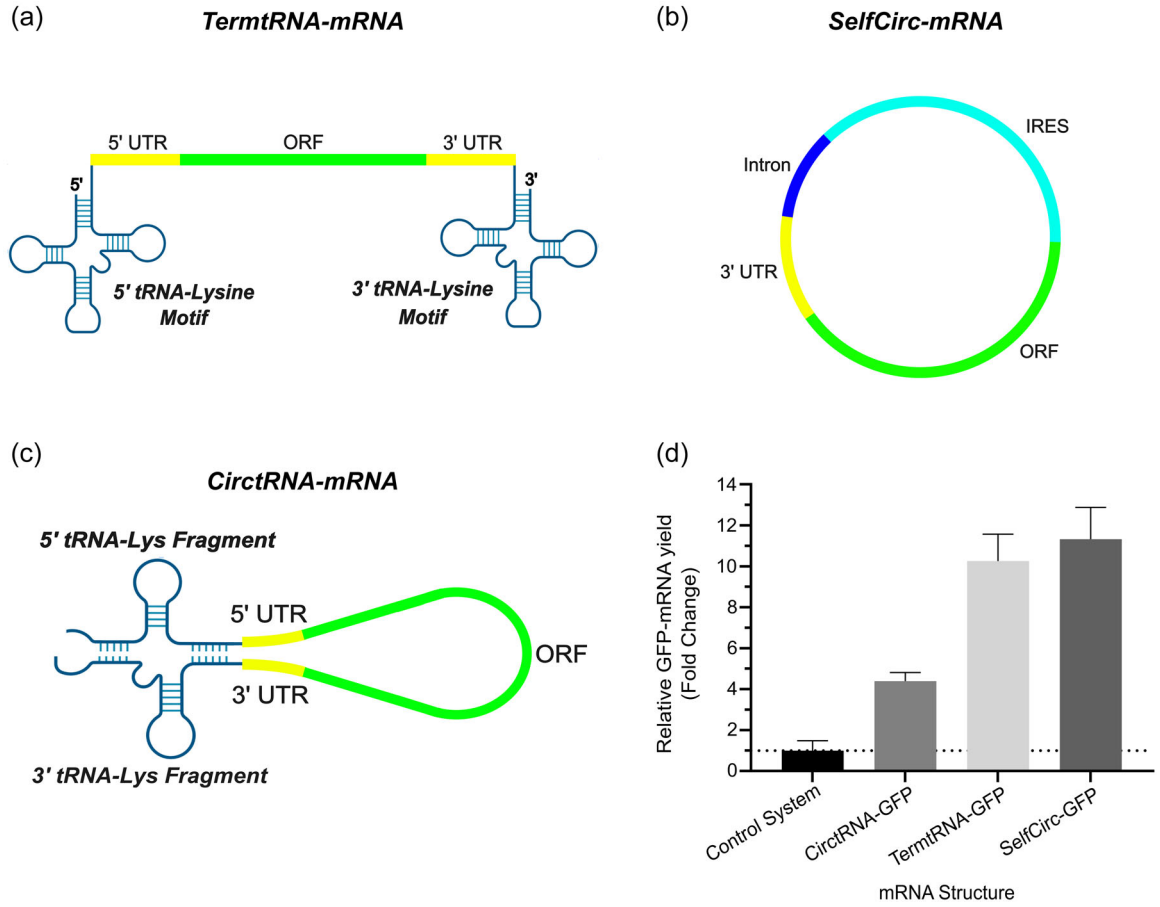

FIGURE 1 mRNA structures were engineered to increase product stability in *Escherichia coli* host-cells by (a) including "scaffold" tRNA-Lysine motifs at both the 5′ and 3′ termini, (b) incorporating ribozyme sequences to promote self-circularization, and (c) inserting component parts of the tRNA-Lysine motif at the 5′ and 3′ termini to facilitate formation of pseudo-circular molecules. Designed elements were synthesized, individually inserted into a GFP-expression plasmid and evaluated in 2.5 h production processes (d). Data are expressed as a fold-change of the production exhibited by the unengineered control system. Values represent the mean + SD of three independent experiments ($n = 3$, each performed in triplicate). GFP, green fluorescent protein; IRES, internal ribosome entry site; ORF, open reading frame; UTR, untranslated region.

mammalian 5′ and 3′ UTRs, including an encoded polyA tail, to permit translation of purified mRNA in human cells. GFP-vectors were transformed into the *E. coli* protein production strain BL21 (DE3) and small-scale mRNA production processes were carried out. Cells were cultured in 5 mL LB broth, before addition of IPTG to induce recombinant mRNA expression in exponential-phase cultures. Total RNA was extracted 150 min after induction of expression and GFP mRNA yields were quantified by using ddPCR to calculate absolute product mRNA copy numbers in 1 ng of total RNA from each sample. Total RNA per cell did not significantly vary when different mRNA constructs were utilized (data not shown), and accordingly differences in GFP mRNA yield were reflective of relative changes in product mRNA accumulation/maintenance. Although we did not specifically measure DNA plasmid copy numbers per cell, we assumed this was unlikely to vary between the different test constructs as all vectors contained the same origin of replication and were approximately equal in size (<10% difference between smallest and largest plasmid).

As shown in Figure 1d, each of the engineered constructs facilitated substantial increases in mRNA product yield, as compared to the standard unengineered control, a linear GFP molecule flanked by *Xenopus* β-globin 5′ and 3′ UTRs. The best performing construct, SelfCirc-mRNA, enhanced GFP mRNA yield by >11-fold, indicating that these circularized molecules were efficiently shielded from RNAse E-mediated product decay. CirctRNA- (4.5-fold increase in product yield compared to control) had a significantly reduced stabilizing effect compared to TermtRNA- (10-fold increase), which may be due to relatively inefficient formation of the tRNA motif in this molecular context. Unlike the tRNA-based elements, SelfCirc-mRNA is also protected from degradation by 3′–5′ exonucleases, which play a relatively minor role in global mRNA decay in *E. coli* but are particularly active on polyadenylated transcripts (Mohanty & Kushner, 2022). Moreover, circular mRNA molecules can be directly utilized in downstream applications without requiring the addition of a cap structure or incorporation of modified nucleotides. Indeed, given its low immunogenicity and high molecular stability, both in

mammalian cells and during product storage (Deviatkin et al., 2023), circular mRNA is considered a promising molecular format for a variety of applications (Bai et al., 2023; Liu et al., 2022; Qu et al., 2022). As circularized mRNA facilitated the highest production yields in *E. coli*, while also being associated with simplified downstream processing requirements, we concluded that this emerging product class was particularly well-suited for an in vivo biomanufacturing system. Accordingly, we focussed further optimization of our platform on enhancing production of SelfCirc-mRNA.

3.2 | Cell, DNA, and media engineering to maximize mRNA product yield

We previously described a whole pathway engineering approach that maximized production of recombinant proteins in Chinese hamster ovary cells, whereby substantial increases in product yield were achieved via coordinated design of the host cell and DNA expression vector components (Brown et al., 2019). We hypothesized that a similar strategy could be applied to mRNA manufacturing in *E. coli* by sequentially improving the system components that determine recombinant product yields, namely the host cell chassis, DNA expression vector, and cell culture media (Sandomenico et al., 2020; Soini et al., 2008; Ziegler et al., 2021). Commercially available *E. coli* strains have been engineered to reduce RNase E activity to levels that enhance recombinant mRNA stability without impacting global mRNA homeostasis (Heyde & Nørholm, 2021; Miroux & Walker, 1996). Although these strains were originally designed to increase production of "easy to express" recombinant proteins, they theoretically provide a highly permissive cell background for synthetic mRNA manufacture. To directly test this, we compared SelfCirc-mRNA production in previously utilized standard BL21 (DE3) (F^-*ompT hsdS*$_B$ (r_B^-, m_B^-) *gal dcm* (DE3)) cells and engineered BL21 Star (DE3) (F^-*ompT hsd*SB (r_B–, m_B–) *gal dcm rne*131 (DE3)) cells. Relative product yields were again quantified by measuring absolute GFP mRNA copy numbers in 1 ng of extracted total RNA, where total RNA per cell was not significantly affected by the utilization of different cell strains, DNA expression constructs or media compositions. As shown in Figure 2a, cells expressing a mutated RNAse E produced ~1.8-fold more GFP mRNA than the unengineered strain, without affecting cell growth rate (data not shown). Although circular mRNA is efficiently protected from RNase E mediated degradation, covalent circularization requires synthesis of the full-length transcript. A reduction in RNase E activity may therefore enhance synthetic mRNA yields by preventing turnover of nascent product mRNA, increasing the pool of mRNA molecules available for circularization. Product yields may be further enhanced by cell engineering strategies that increase the host cell's mRNA biosynthesis (e.g., T7 expression level) and/or cell biomass accumulation capacities.

We rationalized that promoter engineering was unlikely to increase product yields, as the expression plasmid already contained a T7 promoter optimized to maximize recombinant mRNA transcription rates. However, enhancing the number of plasmid copies per cell has previously been shown to enhance manufacture of short dsRNA molecules (Ponchon et al., 2013). Accordingly, we tested the effect of using a pUC origin of replication (Ori), which permits very high plasmid copy numbers per cell (~500–700; Lee et al., 2006; Lin-Chao et al., 1992). As shown in Figure 2b, the use of this element did not increase GFP mRNA yields in BL21 Star cells, as compared to the use of the original Rop-ColE1 Ori, despite that construct only encoding maintenance of ~15–20 copies/cell (Bolivar et al., 1977; Lee et al., 2006). This may be caused by the intrinsic metabolic burden associated with replicating and transcribing very high DNA plasmid loads. It is likely that testing a range of synthetic Oris (Joshi et al., 2022; Rouches et al., 2022) will identify a plasmid copy number "sweet spot" that optimizes the quantity of DNA templates available for product biosynthesis without negatively impacting other desirable cellular bioproduction phenotypes.

Beyond the promoter and the Ori, the final DNA plasmid element that can be engineered is the transcriptional terminator. The original expression plasmid utilized a standard class I intrinsic late T7 terminator, TΦ, however, this is known to encode a termination efficiency of only ~74% (Carter et al., 1981). Replacing TΦ with a previously described novel triple terminator, comprising a combination of T7 TΦ, T3 and *E. coli* rrnBT1 endogenous terminators, enhanced GFP mRNA yields by ~40% (Figure 2b). This triple terminator has been shown to effectively eliminate read-through transcription by T7 RNA Polymerase (Mairhofer et al., 2015). Accordingly, this terminator facilitates enhanced RNA Polymerase recycling efficiency and increases the total biocatalyst time available for productive synthetic mRNA biosynthesis.

Producing high levels of synthetic mRNA may create product titer-limiting burden/bottlenecks in host cell metabolic pathways. We tested the effect of replacing the commonly utilized protein and plasmid production cell culture media LB broth with other commercially available formulations. Terrific Broth and Bacto CD Supreme Fermentation media were investigated as their use of glycerol, as opposed to oligopeptides, as a carbon source has been reported to increase maximum cell culture densities (Kram & Finkel, 2015). However, both media formulations significantly reduced mRNA product titers (Figure 2c), likely due to the lower cell growth rates achieved (data not shown). We also tested supplementation with L-Glutamine, based on the hypothesis that an additional nitrogen source would enhance mRNA biosynthetic capacity by increasing nucleoside biogenesis, however, this did not significantly impact product yields (Figure 2c). Finally, we evaluated the chemical effector design space to identify small molecules that could specifically enhance mRNA production in *E. coli*. The most promising chemicals identified were a range of RNAse E inhibitors that reduce enzyme activity via interactions with the N-terminal domain. However, only one of these inhibitors was commercially available, and accordingly we tested the effect of supplementing LB media with 3-(4-Hydroxy-5-isopropyl-6-oxo-1,6-dihydro-pyrimidin-2-ylsulfanyl)-propionic acid (AS2). It was determined that 2 mM AS2 was the optimal concentration for maximizing mRNA maintenance in the cell chassis (Supporting Information: Figure 1), which has previously

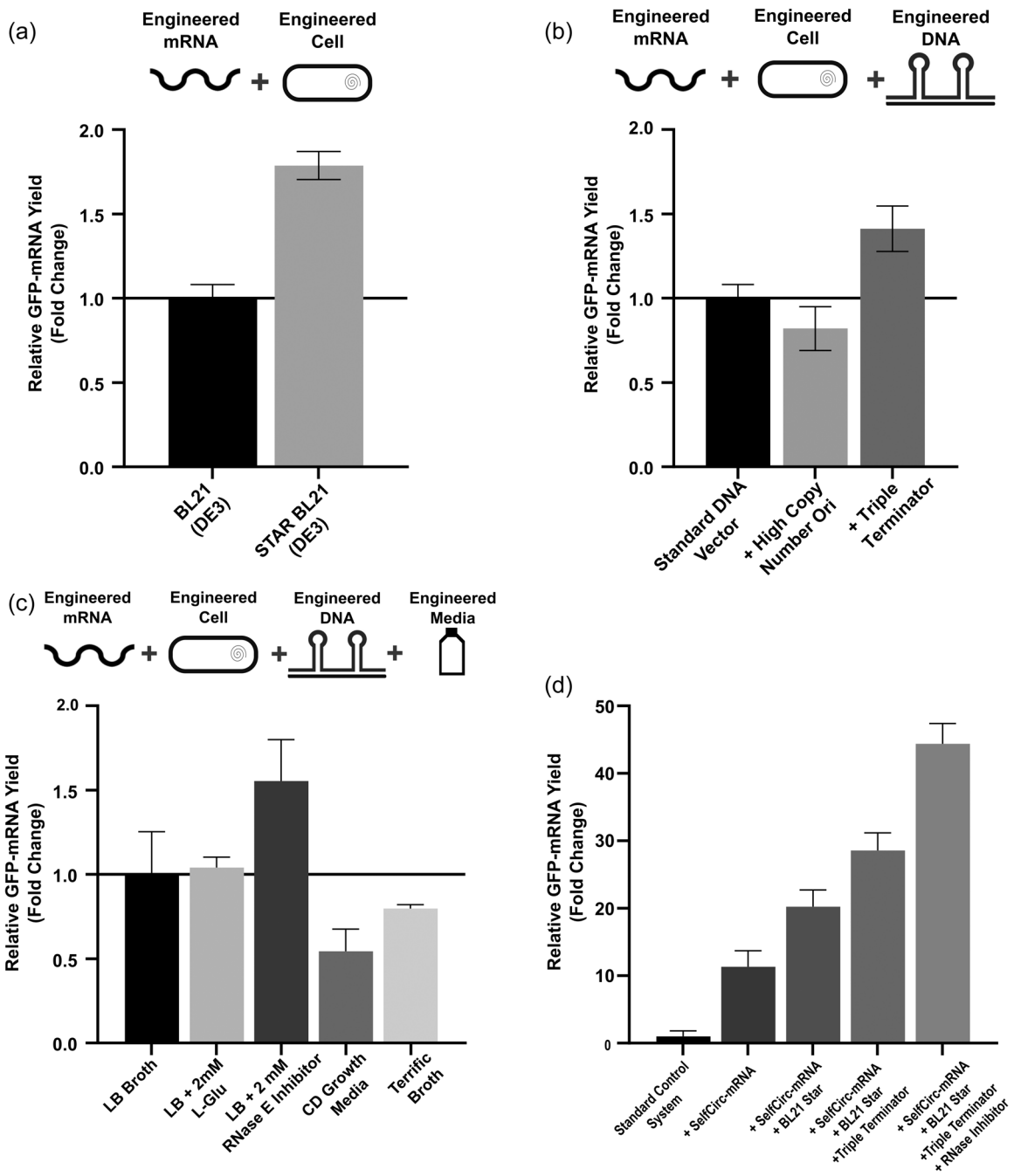

FIGURE 2 mRNA manufacturing platform components were sequentially optimized by evaluating the function of (a) engineered host cell chassis, (b) synthetic DNA expression vectors, and (c) designed cell culture media formulations. The relative performance of engineered systems was evaluated in 2.5 h production processes. The additive impact of each engineering step on overall product yield is shown in (d). Data are expressed as a fold-change of the production achieved using standard control components. Values represent the mean + SD of three independent experiments ($n = 3$, each performed in triplicate). In all panels, the expressed product is SelfCirc-GFP (see Figure 1); the effect of whole system engineering on manufacture of TermtRNA-GFP is shown in Supporting Information: Figure 2. GFP, green fluorescent protein.

been shown to reduce RNase E activity in *E. coli* by > 80% (Kime et al., 2015; Mardle et al., 2020). Utilizing AS2 at this concentration increased mRNA yield by ~50% (Figure 2c), where higher concentrations reduced cellular productivity. While a similar increase in titer may be possible via BL21 STAR cell engineering to further attenuate RNAse E activity, AS2 supplementation offers a robust mechanism to precisely optimize the synthetic mRNA-RNAse E interactome in a product-specific manner. Similarly, the use of AS2 in combination with a mutated RNAse E permits use of inhibitor concentrations with reduced off-target effects on the host cell.

The optimal combination of engineered mRNA construct (SelfCirc-mRNA), DNA expression plasmid (Triple terminator), cell

host (BL21 STAR), and media formulation (LB + AS2), facilitated a 44× increase in mRNA product yield, compared to the standard control system (a linear GFP molecule flanked by *Xenopus* β-globin 5′ and 3′ UTRs, utilizing a standard class I T7 terminator, produced in BL21 (DE3) cells without addition of RNAse inhibitor, Figure 2d). CGE analysis confirmed that product mRNA was full-length and constituted a substantial proportion of total cellular RNA (>20%, compared to <1% for the standard control system; Figure 3a). Moreover, high yields of full-length synthetic mRNA were maintained when the relatively small GFP coding sequence (720 nt) was substituted for Cypridina Luciferase (1662 nt) or SARS-COV-2 Spike Protein (3783 nt) (Figure 3b), demonstrating that the engineered in vivo biomanufacturing system can produce larger, more complex molecules. Finally, using oligo-dT magnetic beads, we validated that achieved increases in product yield were maintained following small-scale purification processes (Figure 3c). This also demonstrates that mRNA manufactured in an *E. coli* cell-host can be purified using simple low-tech methodologies, facilitated by the absence of abundant endogenous mRNAs with Poly(A) tails >5 nucleotides in length (Laalami et al., 2014; Mohanty & Kushner, 2019).

3.3 | Mechanistic dissection of synthetic mRNA production in *E. coli* host cell chassis

To understand how *E. coli* host cells utilize available biosynthetic capacity for mRNA production, we profiled cell biomass, total RNA, and product mRNA accumulation/maintenance during a 6 h

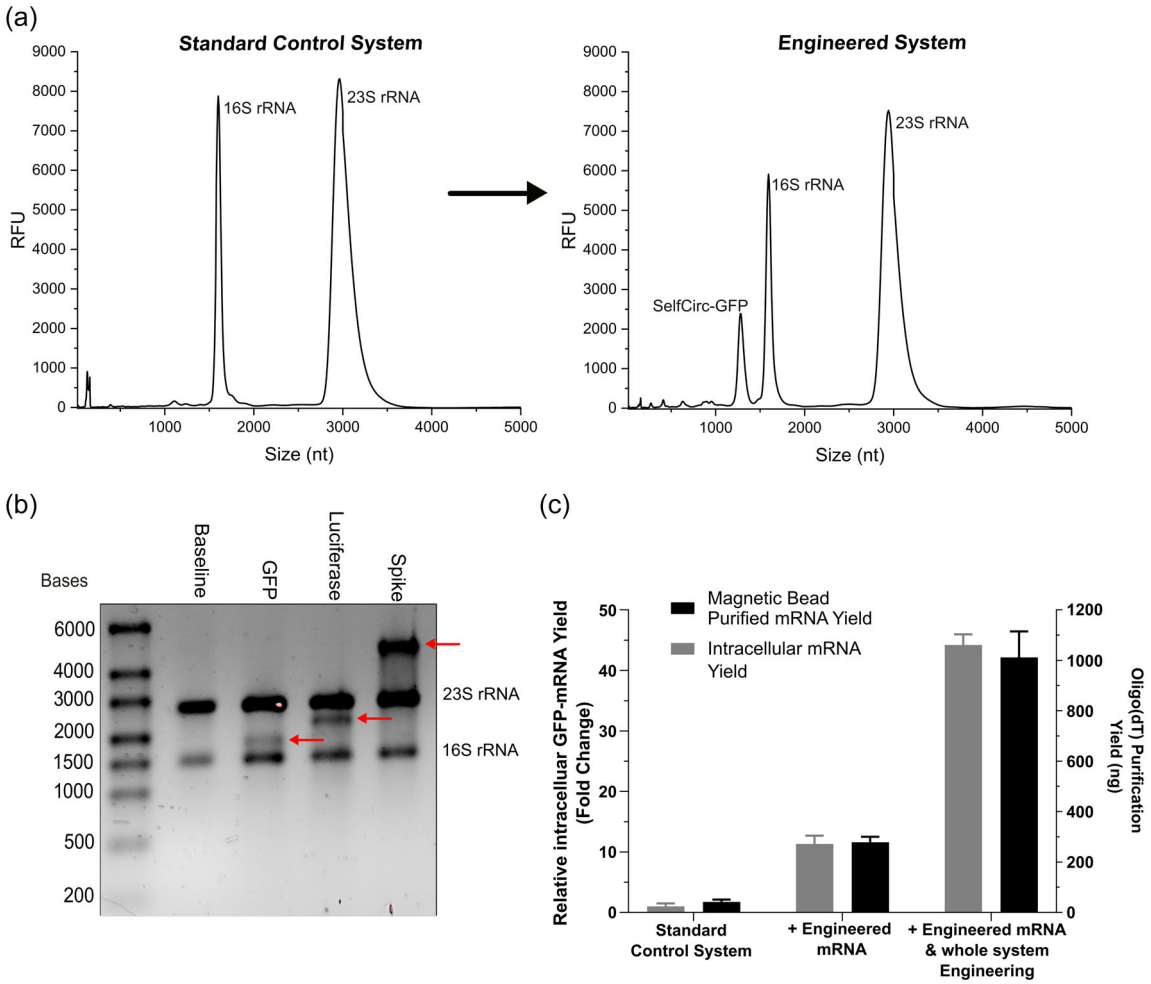

FIGURE 3 (a) Capillary electropherograms of total RNA isolated from GFP-mRNA biomanufacturing systems comprising either (i) standard control components, or (ii) an optimal combination of engineered mRNA construct, DNA expression plasmid, cell host and media formulation (engineered system, see Figure 2). (b) Gel electrophoresis analysis of total RNA isolated from engineered systems producing GFP, SARS-COV-2 Spike, and Cypridina Luciferase mRNA molecules. Full-length product mRNA molecules are highlighted by red arrows; molecule sizes are enlarged due to the presence of IRES and Intron elements in SelfCirc-mRNA (see Figure 1). (c) Comparison of relative GFP-mRNA yields obtained from standard control and engineered systems, quantified before (intracellular) and after purification using oligo-dT magnetic beads. Intracellular yields are expressed as a fold-change of the product yield obtained using the Standard control system. Values represent the mean + SD of three independent experiments ($n = 3$, each performed in triplicate). GFP, green fluorescent protein; IRES, internal ribosome entry site.

manufacturing time course. We utilized the previously optimized cell-DNA-media composition (see Figure 2) to manufacture SARS-COV-2 Spike Protein mRNA. To evaluate mechanistic differences between biosynthesis of circular and linear molecules, we separately manufactured SelfCirc- and TermtRNA-mRNA products. With respect to the latter, we confirmed that the optimal BL21 STAR-Triple terminator-LB(AS2) system combination permitted a 36-fold increase in TermtRNA-GFP yields as compared to the standard control system (a linear GFP molecule flanked by *Xenopus* β-globin 5′ and 3′ UTRs, utilizing a standard class I T7 terminator, produced in BL21 (DE3) cells without addition of RNAse inhibitor; see Supporting Information: Figure 2), similar to the 44-fold increase achieved for SelfCirc-GFP.

As shown in Figure 4a, manufacture of circular and linear synthetic mRNA products induced a significant metabolic burden on the host cell, where producer cells accumulated significantly less biomass over the 6 h timecourse. Indeed, these cells exhibited a 25% reduction in cell specific growth rate during the first 2 h postexpression induction (Figure 4b). Moreover, the final maximum cell density achieved was ~50% lower for producer cells, as compared to nonproducers, associated with a ~35% reduction in the integral of cell concentration (cumulative cell hours; Figure 4b). This indicates that producing substantial amounts of synthetic mRNA forces the cell to reallocate biosynthetic capacity away from cell biomass generation activities. Accordingly, approaches to overcome product biosynthesis-associated burden represent a potentially effective way to enhance total biocatalyst activity and further increase product yields. This may be achieved through optimization of expression induction kinetics, genetic engineering, and/or directed evolution strategies (Al'abri et al., 2022; Badran & Liu, 2015; Esvelt et al., 2011). In addition to efforts to optimize how host cells manage the competing objectives of product and cell biomass generation/maintenance, the most significant increases in mRNA yield will presumably be achieved via implementation of fed-batch bioreactor processes that facilitate substantial increases in maximum achievable cell densities (Glazyrina et al., 2010; Scheel et al., 2021).

As shown in Figure 4c, total RNA synthesized per cell was stable throughout the production process, at ~60 fg/cell, despite Spike Protein-mRNA accumulating over time (Figure 4d). This is likely due to feedback mechanisms that act to maintain intracellular concentrations of key macromolecules within relatively narrow concentration ranges (Radoš et al., 2022). Accordingly, accumulation of highly stable product-mRNA forces the cell to reduce biosynthesis and/or induce degradation of endogenous RNA species, with potential associated off-target effects on desirable bioproduction phenotypes such as cell growth rate. These RNA homeostasis mechanisms place a theoretical limit on the total quantity of product-mRNA that can be maintained per cell, above which concentrations of key endogenous RNA molecules will become critically limiting leading to cell death and/or downregulation of product expression. Indeed, as shown in Figure 4d, intracellular concentrations of Spike Protein-mRNA peaked at 4 h, before decreasing slightly at 6 h. At 4 h, SelfCirc-Spike accounted for ~28% of total RNA mass in the host-cell, which is likely approaching the maximum achievable concentration. Although not a direct comparison, during recombinant protein expression in *E. coli*, efficiently translated product molecules typically account for up to 50% of intracellular protein mass (Jia & Jeon, 2016; Studier & Moffatt, 1986). We concluded that engineering efforts to further enhance intracellular product maintenance are unlikely to be beneficial, and instead should focus on maximizing product accumulation rates. For SelfCirc-Spike, cell specific productivity (product-mRNA produced per cell per hour) was relatively constant throughout the first 4 h of the production process, at ~5 fg/cell/h, equating to ~10% of total cellular RNA biosynthetic activity during this time period. DNA vector engineering, for example, T7 promoter re-design, may increase synthetic mRNA generation rates, facilitating cells to reach the maximum intracellular product-mRNA concentration level more quickly, permitting shorter production processes with associated benefits in cost and manufacturing flexibility (i.e., ability to rapidly switch between manufacture of different products).

CGE analysis clearly shows that product mRNA accumulates intracellularly over time (Figure 4f,g). These data exemplify that engineered product molecules are successfully protected from nuclease-mediated decay to the extent that product formation rate considerably exceeds that of product degradation. This facilitates intracellular maintenance over multihour time periods, as compared to the turnover kinetics of endogenous *E. coli* mRNA molecules that typically exhibit half-lives of ~5 min (Bernstein et al., 2002; Mohanty & Kushner, 2022). Moreover, the presence of a single sharp peak at each sampling point indicates that the cell factory is producing full-length Spike Protein-mRNA that is subject to minimal degradation events. Accordingly, (i) further system engineering to disrupt the *E. coli* degradasome-synthetic mRNA interactome is not required, and (ii) *E. coli* is capable of synthesizing homogenous populations of large mRNA molecules, thereby simplifying downstream processing steps. As expected, higher titers were obtained for SelfCirc-Spike than TermtRNA-Spike, where maximum achieved yields were 15 and 10 mg/L, respectively (Figure 4e). As discussed, we anticipate that significant increases in product yields will be obtained via further DNA/cell/media engineering to increasecell specific productivity. For example, a co-ordinated strategy of gene overexpression and gene knockdown could be employed to maximize product synthesis capacity, optimize metabolic pathways, and minimize product turnover rates, similar to what has been achieved for plasmid DNA manufacture in *E. coli* (Borja et al., 2012; Jaén et al., 2019; Soto et al., 2011). Beyond this, the maximum cell density could be increased by orders of magnitude by employing optimized fed-batch bioreactor processes. Indeed, given that these processes typically facilitate maximum cell densities >100× higher than the shake-flask batch processes employed in this study, we anticipate that process intensification will permit g/L mRNA titers, as is standard for recombinant protein production in *E. coli*. Although we note that this will likely require optimization of product expression induction kinetics to create manufacturing processes with distinct multiday biomass accumulation and multihour mRNA production phases.

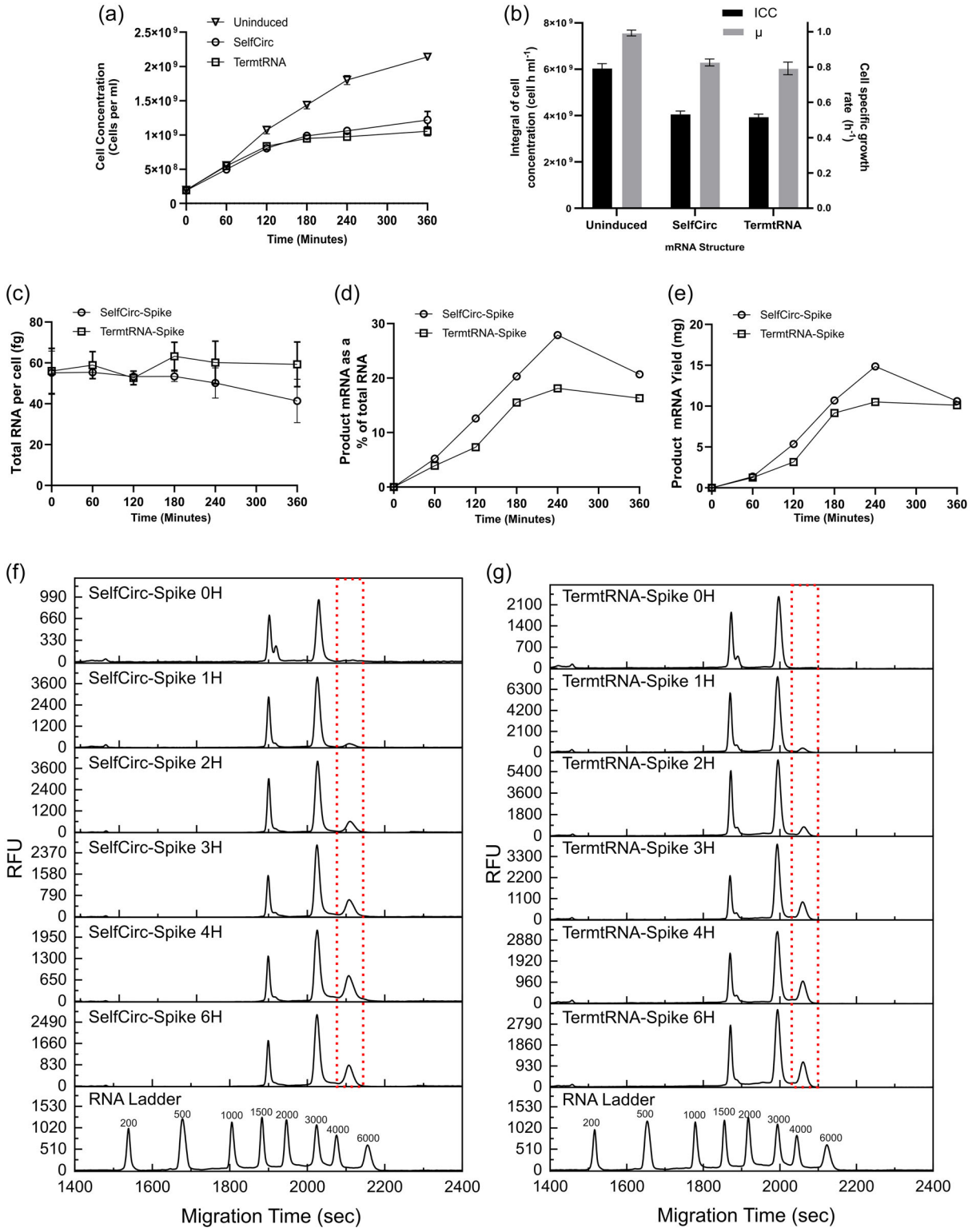

FIGURE 4 SelfCirc-Spike and TermtRNA-Spike were produced in biomanufacturing systems comprising an optimal combination of engineered host cell, DNA plasmid and cell culture media (see Figure 2). Growth of nonproducer (uninduced) and producer cells was measured at 1 h intervals during 6 h production processes (a), to calculate integral cell concentration (ICC) and cell specific growth rate (μ) values (b). Total RNA (c) and product mRNA (e) yields were also measured at 1 h intervals, and the relative proportion of host cell RNA comprising Spike-mRNA molecules was quantified (d). Total RNA samples from each measured timepoint were analyzed by capillary gel electrophoresis; dashed red boxes on capillary electropherograms highlight SelfCirc-Spike (f) and TermtRNA-Spike (g) product accumulating over time. In (a)–(c), values represent the mean ± SD of three independent experiments; (d)–(g) show data from a single representative capillary gel electrophoresis timecourse analysis.

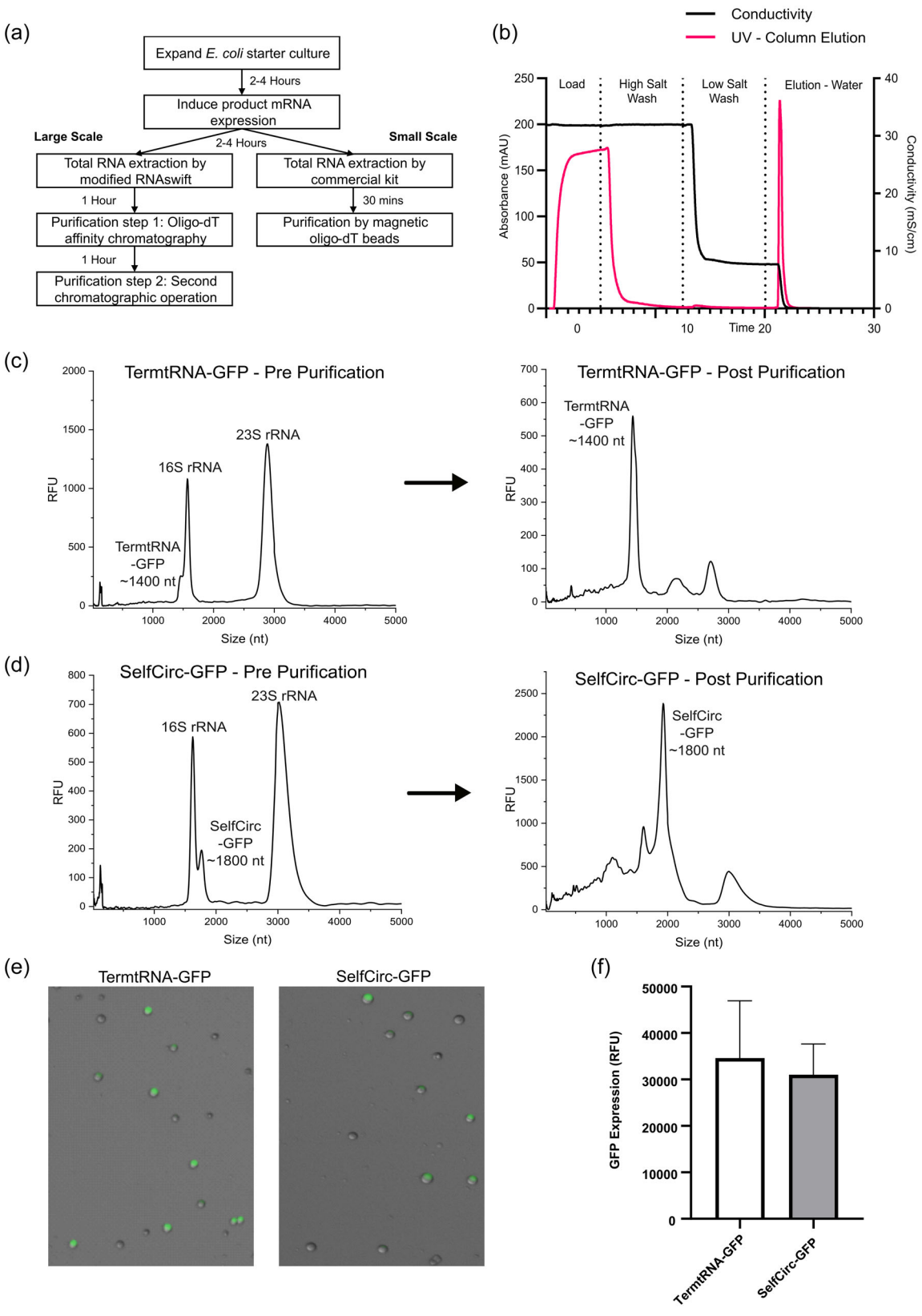

FIGURE 5 (a) Simplified process flow diagram for large-scale and small-scale in vivo mRNA production. (b) Typical chromatogram from oligo-d(T) affinity chromatography purification of product mRNA manufactured in *Escherichia coli*. (c) and (d) Capillary electropherograms showing purification of TermtRNA-GFP (c) and SelfCirc-GFP (d) products using oligo-d(T) affinity chromatography. (e) and (f) mRNA products manufactured in *E. coli* were purified and transfected into human embryonic kidney cells. Twenty-four hours posttransfection, GFP protein expression was measured by fluorescent cell imaging (e) and fluorescent plate reader analysis (f). Values in F represent the mean + SD of three independent experiments ($n = 3$, each performed in triplicate). GFP, green fluorescent protein.

3.4 | Synthetic mRNA produced in *E. coli* can be purified and is functional in human cells

To exemplify the utility of our *E. coli*-based system for mRNA synthesis we manufactured GFP-mRNA in 4 h 1 L production processes, where maximal cell densities reached ~1×10^9 cells/mL. The first purification step required is total RNA extraction from host cell factories. While this can be achieved with commercial kits when production scales are <1 mL, larger volumes require a scalable cost-efficient procedure. To achieve this, we adapted the RNASwift method previously described by Nwokeoji et al. (2016) for extraction of dsRNA products from *E. coli* that utilizes NaCL and SDS to lyse cells and precipitate macromolecular contaminants. To maximize both total RNA yield and RNA quality, we (i) introduced a lysozyme digestion step upstream of RNASwift, (ii) lowered the lysis incubation temperature from 90°C to 65°C, and (iii) added an ethanol precipitation step downstream of RNASwift. Using this modified RNASwift unit operation we were able to routinely obtain large yields (10 mg per 0.5 g wet cell mass) of high-quality total RNA (RNA integrity numbers > 9.5, as determined by CGE).

While small amounts of product-mRNA can be purified from total RNA using oligo-dT magnetic beads (see Figure 3c), larger quantities require chromatographic operations. To show that mRNA manufactured in *E. coli* can be purified using a liquid chromatography separation step, we utilized a 1 mL monolithic oligo-dT(18) column in combination with an AKTA PCC system. Figure 5b shows a chromatogram representative of this purification process, indicating conductivity as a measure of salt concentration, and the UV trace of material eluted from the column. CGE analysis of pre- and postpurification samples showed that both SelfCirc-GFP and TermtRNA-GFP molecules could be efficiently purified by an affinity-capture chromatographic unit operation (Figure 5c,d). However, TermtRNA-GFP was isolated at much high purity, 71% as compared to 38% for SelfCirc-GFP, where SelfCirc-GFP samples showed a considerable wide peak of impurities representing ~30% of total RNA. This may be due to SelfCirc-GFP molecules having considerably smaller polyA tails than TermtRNA-GFP species, 50 and 120 nt, respectively, preventing use of elution conditions that deliver both high yield and high purity. Further mRNA/DNA engineering to increase the encoded polyA tail length should permit product isolation with reduced process/product related impurities. Either way, for both molecule-formats, it is clear that for most applications a second chromatographic unit operation would be needed to achieve requisite purity profiles, such as a size-exclusion chromatography step. The use of two chromatographic unit operations is standard for purification of other high-value macromolecules, including recombinant proteins and IVT-derived mRNA (Fan et al., 2023; Rosa et al., 2021; Sripada et al., 2022). Additionally, substantial increases in purity, as would be required for clinical contexts, could be achieved by (i) full optimization of chromatographic critical process parameters, such as buffer conditions and flow rates, and (ii) minimization of product degradation by producing mRNA under good manufacturing practice compliant conditions. Finally, for in vivo applications, it is essential that fully optimized two-step chromatographic purification processes remove host cell DNA and endotoxin impurities, as is routinely achieved for protein and DNA products manufactured in *E. coli* (Kiesewetter et al., 2023). A simplified conceptual process flow diagram for large-scale and small-scale in vivo mRNA production processes is shown in Figure 5a.

Finally, to validate that mRNA products manufactured in *E. coli* were functional in mammalian cells, we transfected purified SelfCirc-GFP and TermtRNA-GFP into human embryonic kidney (HEK) cells. While SelfCirc-GFP contains an internal ribosome binding site (IRES), obviating the need for postpurification processing, TermtRNA-GFP required the enzymatic addition of a Cap-0 structure to enable translation initiation. As shown in Figure 5e,f, both synthetic mRNA molecular formats were translatable in HEK cells, facilitating similar levels of GFP protein expression. Translational efficiency of SelfCirc-GFP molecules would likely be further enhanced via determination and selection of optimal IRES elements (Wesselhoeft et al., 2018). Indeed, this may provide a route to encode cell-type specificity into mRNA gene therapeutics (Plank et al., 2013).

4 | CONCLUDING REMARKS

The in vivo mRNA manufacturing system we have presented here can be utilized to produce synthetic mRNA molecules for a wide range of research and commercial applications. Although we have demonstrated for the first time that functional mammalian mRNA can be produced at high-yields in *E. coli* cell factories, widespread adoption of this platform requires further optimization of both (i) downstream processing steps to increase product purities and (ii) upstream processes to maximize product titers by enhancing cell specific productivity and cell biomass accumulation/maintenance. Additionally, the mRNA manufactured in such optimized processes will need to be fully profiled to validate required critical quality attributes such as impurity levels and integrity of full-length primary sequences (Jackson et al., 2020). Indeed, synthetic mRNA manufactured in the "natural" context of a cellular environment may potentially offer advantages (Claassens et al., 2019) with respect to product quality by reducing formation of product-related impurities associated with IVT-processes such as dsRNA and abortive transcripts (e.g., the *E. coli* cell chassis contains RNAse III which efficiently degrades dsRNA [Court et al., 2013]). Although purifying mRNA from cellular systems is also complicated by requirements to remove process-related impurities such as endotoxin and host cell nucleic acids, this is routinely achieved for DNA and protein products using similar unit operations as those currently employed for IVT-based systems (Rosa et al., 2021; Youssef et al., 2023). Assuming the cell specific productivity observed in this study is maintained in intensified fed-batch bioreactor processes, *E. coli*-based systems should facilitate at least similar product yields to traditional IVT-based processes (~5 g/L, Kis et al., 2021), and at significantly reduced costs by removing requirements for highly purified input material components (van de Berg et al., 2021). However, definitively elucidating the relative

potential advantages/disadvantages compared to IVT will require rigorous testing of a fully optimized system in industrially relevant processes, with associated techno-economic assessment. While we anticipate that the developed system will be particularly suitable for production of circular mRNA products, a current drawback relative to IVT is the requirement for postextraction enzymatic capping of linear molecules. Its utility for manufacturing such products would be significantly enhanced by optimizing co-expression of a T7-Capping enzyme fusion protein (Qin et al., 2023) to enable synthesis of capped mRNA species in *E. coli*. Similarly, co-expression of nucleotide-modifying enzymes, such as Psuedouridine synthetase (Carlile et al., 2019), would permit production of linear mRNA products with required immunostimulatory properties for therapeutic applications.

The potential utility of microbial cell factories for large-scale mRNA manufacturing is being increasingly recognized. Indeed, earlier this year saw announcements of plans to develop commercial cell-based mRNA production processes using eukaryotic cell-hosts. The availability of such platforms will become increasingly critical in coming years as product lines begin to diversify (e.g., adoption of more complex molecular formats) and the scale of global mRNA manufacturing continues to increase. By engineering the core components of an *E. coli*-based mRNA production system, this study has added a novel technology to the mRNA manufacturing solution space, providing flexibility to achieve context- and/or application-specific design criteria.

AUTHOR CONTRIBUTIONS

Edward Curry: Conceptualization; methodology; analysis; investigation; manuscript preparation. **George Muir**: Investigation; analysis. **Jixin Qu**: Investigation; analysis. **Zoltan Kis**: Investigation; analysis. **Martyn Hulley**: Conceptualization; analysis. **Adam Brown**: Conceptualization; methodology; analysis; manuscript preparation; funding acquisition.

ACKNOWLEDGMENTS

This study was supported by AstraZeneca and the Biotechnology and Biological Sciences Research Council (Grant No. BB/T508664/1).

CONFLICT OF INTEREST STATEMENT

The authors declare no conflict of interest.

DATA AVAILABILITY STATEMENT

The data that support the findings of this study are available from the corresponding author upon reasonable request.

ORCID

Edward Curry http://orcid.org/0000-0002-5123-8866
Adam Brown http://orcid.org/0000-0002-3290-4560

REFERENCES

Agostinetto, R., Rossi, M., Dawson, J., Lim, A., Simoneau, M. H., Boucher, C., Valldorf, B., Ross-Gillespie, A., Jardine, J. G., Sok, D., Burton, D. R., Hassell, T., Broly, H., Palinsky, W., Dupraz, P., Feinberg, M., & Dey, A. K. (2022). Rapid cGMP manufacturing of COVID-19 monoclonal antibody using stable CHO cell pools. *Biotechnology and Bioengineering*, *119*, 663–666.

Al'abri, I. S., Haller, D. J., Li, Z., & Crook, N. (2022). Inducible directed evolution of complex phenotypes in bacteria. *Nucleic Acids Research*, *50*, e58.

Baden, L. R., El Sahly, H. M., Essink, B., Kotloff, K., Frey, S., Novak, R., Diemert, D., Spector, S. A., Rouphael, N., Creech, C. B., McGettigan, J., Khetan, S., Segall, N., Solis, J., Brosz, A., Fierro, C., Schwartz, H., Neuzil, K., Corey, L., … Zaks, T. (2021). Efficacy and safety of the mRNA-1273 SARS-CoV-2 vaccine. *New England Journal of Medicine*, *384*, 403–416.

Badran, A. H., & Liu, D. R. (2015). In vivo continuous directed evolution. *Current Opinion in Chemical Biology*, *24*, 1–10.

Bae, D., Hyeon, H., Shin, E., Yeom, J. H., & Lee, K. (2023). Relaxed cleavage specificity of hyperactive variants of *Escherichia coli* RNase E on RNA I. *Journal of Microbiology*, *61*, 211–220.

Bai, Y., Liu, D., He, Q., Liu, J., Mao, Q., & Liang, Z. (2023). Research progress on circular RNA vaccines. *Frontiers in Immunology*, *13*, 1–12.

van de Berg, D., Kis, Z., Behmer, C. F., Samnuan, K., Blakney, A. K., Kontoravdi, C., Shattock, R., & Shah, N. (2021). Quality by design modelling to support rapid RNA vaccine production against emerging infectious diseases. *NPJ Vaccines*, *6*, 65.

Bernstein, J. A., Khodursky, A. B., Lin, P. H., Lin-Chao, S., & Cohen, S. N. (2002). Global analysis of mRNA decay and abundance in *Escherichia coli* at single-gene resolution using two-color fluorescent DNA microarrays. *Proceedings of the National Academy of Sciences*, *99*, 9697–9702.

Bolivar, F., Rodriguez, R. L., Greene, P. J., Betlach, M. C., Heyneker, H. L., Boyer, H. W., Crosa, J. H., & Falkow, S. (1977). Construction and characterization of new cloning vehicles. II. A multipurpose cloning system. *Gene*, *2*, 95–113.

Borja, G. M., Meza Mora, E., Barrón, B., Gosset, G., Ramírez, O. T., & Lara, A. R. (2012). Engineering *Escherichia coli* to increase plasmid DNA production in high cell-density cultivations in batch mode. *Microbial Cell Factories*, *11*, 132.

Börner, J., Friedrich, T., Bartkuhn, M., & Klug, G. (2023). Ribonuclease E strongly impacts bacterial adaptation to different growth conditions. *RNA Biology*, *20*, 120–135.

Breda, L., Papp, T. E., Triebwasser, M. P., Yadegari, A., Fedorky, M. T., Tanaka, N., Abdulmalik, O., Pavani, G., Wang, Y., Grupp, S. A., Chou, S. T., Ni, H., Mui, B. L., Tam, Y. K., Weissman, D., Rivella, S., & Parhiz, H. (2023). In vivo hematopoietic stem cell modification by mRNA delivery. *Science*, *381*, 436–443.

Brown, A. J., Gibson, S. J., Hatton, D., Arnall, C. L., & James, D. C. (2019). Whole synthetic pathway engineering of recombinant protein production. *Biotechnology and Bioengineering*, *116*, 375–387.

Callaghan, A. J., Marcaida, M. J., Stead, J. A., McDowall, K. J., Scott, W. G., & Luisi, B. F. (2005). Structure of *Escherichia coli* RNase E catalytic domain and implications for RNA turnover. *Nature*, *437*, 1187–1191.

Carlile, T. M., Martinez, N. M., Schaening, C., Su, A., Bell, T. A., Zinshteyn, B., & Gilbert, W. V. (2019). mRNA structure determines modification by pseudouridine synthase 1. *Nature Chemical Biology*, *15*, 966–974.

Carter, A. D., Morris, C. E., & McAllister, W. T. (1981). Revised transcription map of the late region of bacteriophage T7 DNA. *Journal of Virology*, *37*, 636–642.

Claassens, N. J., Burgener, S., Vögeli, B., Erb, T. J., & Bar-Even, A. (2019). A critical comparison of cellular and cell-free bioproduction systems. *Current Opinion in Biotechnology*, *60*, 221–229.

Court, D. L., Gan, J., Liang, Y. H., Shaw, G. X., Tropea, J. E., Costantino, N., Waugh, D. S., & Ji, X. (2013). RNase III: Genetics and function; structure and mechanism. *Annual Review of Genetics*, *47*, 405–431.

Delgado-Martín, J., & Velasco, L. (2021). An efficient dsRNA constitutive expression system in *Escherichia coli*. *Applied Microbiology and Biotechnology*, *105*, 6381–6393.

Deviatkin, A. A., Simonov, R. A., Trutneva, K. A., Maznina, A. A., Soroka, A. B., Kogan, A. A., Feoktistova, S. G., Khavina, E. M., Mityaeva, O. N., & Volchkov, P. Y. (2023). Cap-independent circular mRNA translation efficiency. *Vaccines*, *11*, 238.

Esquerré, T., Moisan, A., Chiapello, H., Arike, L., Vilu, R., Gaspin, C., Cocaign-Bousquet, M., & Girbal, L. (2015). Genome-wide investigation of mRNA lifetime determinants in *Escherichia coli* cells cultured at different growth rates. *BMC Genomics*, *16*, 275.

Esvelt, K. M., Carlson, J. C., & Liu, D. R. (2011). A system for the continuous directed evolution of biomolecules. *Nature*, *472*, 499–503.

Fan, J., Sripada, S. A., Pham, D. N., Linova, M. Y., Woodley, J. M., Menegatti, S., Boi, C., & Carbonell, R. G. (2023). Purification of a monoclonal antibody using a novel high-capacity multimodal cation exchange nonwoven membrane. *Separation and Purification Technology*, *317*, 123920.

Gan, L. M., Lagerström-Fermér, M., Carlsson, L. G., Arfvidsson, C., Egnell, A. C., Rudvik, A., Kjaer, M., Collén, A., Thompson, J. D., Joyal, J., Chialda, L., Koernicke, T., Fuhr, R., Chien, K. R., & Fritsche-Danielson, R. (2019). Intradermal delivery of modified mRNA encoding VEGF-A in patients with type 2 diabetes. *Nature Communications*, *10*, 871.

Gholamalipour, Y., Karunanayake Mudiyanselage, A., & Martin, C. T. (2018). 3′ end additions by T7 RNA polymerase are RNA self-templated, distributive and diverse in character—RNA-Seq analyses. *Nucleic Acids Research*, *46*, 9253–9263.

Glazyrina, J., Materne, E. M., Dreher, T., Storm, D., Junne, S., Adams, T., Greller, G., & Neubauer, P. (2010). High cell density cultivation and recombinant protein production with *Escherichia coli* in a rocking-motion-type bioreactor. *Microbial Cell Factories*, *9*, 42.

Heyde, S. A. H., & Nørholm, M. H. H. (2021). Tailoring the evolution of BL21(DE3) uncovers a key role for RNA stability in gene expression toxicity. *Nature Communications*, *21*, 1–9.

Jackson, N. A. C., Kester, K. E., Casimiro, D., Gurunathan, S., & DeRosa, F. (2020). The promise of mRNA vaccines: A biotech and industrial perspective. *NPJ Vaccines*, *5*, 11.

Jaén, K. E., Velázquez, D., Sigala, J. C., & Lara, A. R. (2019). Design of a microaerobically inducible replicon for high-yield plasmid DNA production. *Biotechnology and Bioengineering*, *116*, 2514–2525.

Jia, B., & Jeon, C. O. (2016). High-throughput recombinant protein expression in *Escherichia coli*: Current status and future perspectives. *Open Biology*, *6*, 160196.

Jiang, Z., & Dalby, P. A. (2023). Challenges in scaling up AAV-based gene therapy manufacturing. *Trends in Biotechnology*, *41*, 1268–1281.

Joshi, S. H. N., Yong, C., & Gyorgy, A. (2022). Inducible plasmid copy number control for synthetic biology in commonly used *E. coli* strains. *Nature Communications*, *13*, 6691.

Kiesewetter, A., Gupta, A., Heinen-Kreuzig, A., Greenhalgh, T., & Stein, A. (2023). Improved endotoxin removal using ecofriendly detergents for intensified plasmid capture. *Biotechnology Progress*, *39*, e3375.

Kime, L., Vincent, H. A., Gendoo, D. M. A., Jourdan, S. S., Fishwick, C. W. G., Callaghan, A. J., & McDowall, K. J. (2015). The first small-molecule inhibitors of members of the ribonuclease E family. *Scientific Reports*, *5*, 8028.

Kis, Z., Kontoravdi, C., Shattock, R., & Shah, N. (2021). Resources, production scales and time required for producing RNA vaccines for the global pandemic demand. *Vaccines*, *9*, 1–14.

Kram, K. E., & Finkel, S. E. (2015). Rich medium composition affects *Escherichia coli* survival, glycation, and mutation frequency during long-term batch culture. *Applied and Environmental Microbiology*, *81*, 4442–4450.

Laalami, S., Zig, L., & Putzer, H. (2014). Initiation of mRNA decay in bacteria. *Cellular and Molecular Life Sciences*, *71*, 1799–1828.

Lee, C., Kim, J., Shin, S. G., & Hwang, S. (2006). Absolute and relative QPCR quantification of plasmid copy number in *Escherichia coli*. *Journal of Biotechnology*, *123*, 273–280.

Leppek, K., Byeon, G. W., Kladwang, W., Wayment-Steele, H. K., Kerr, C. H., Xu, A. F., Kim, D. S., Topkar, V. V., Choe, C., Rothschild, D., Tiu, G. C., Wellington-Oguri, R., Fujii, K., Sharma, E., Watkins, A. M., Nicol, J. J., Romano, J., Tunguz, B., Diaz, F., … Das, R. (2022). Combinatorial optimization of mRNA structure, stability, and translation for RNA-based therapeutics. *Nature Communications*, *13*, 1536.

Lin-Chao, S., Chen, W. T., & Wong, T. T. (1992). High copy number of the pUC plasmid results from a Rom/Rop-suppressible point mutation in RNA II. *Molecular Microbiology*, *6*, 3385–3393.

Liu, X., Zhang, Y., Zhou, S., Dain, L., Mei, L., & Zhu, G. (2022). Circular RNA: An emerging frontier in RNA therapeutic targets, RNA therapeutics, and mRNA vaccines. *Journal of Controlled Release*, *348*, 84–94.

Ma, Z. Z., Zhou, H., Wei, Y. L., Yan, S., & Shen, J. (2020). A novel plasmid–*Escherichia coli* system produces large batch dsRNAs for insect gene silencing. *Pest Management Science*, *76*, 2505–2512.

Mairhofer, J., Wittwer, A., Cserjan-Puschmann, M., & Striedner, G. (2015). Preventing T7 RNA polymerase read-through transcription—A synthetic termination signal capable of improving bioprocess stability. *ACS Synthetic Biology*, *4*, 265–273.

Mardle, C. E., Goddard, L. R., Spelman, B. C., Atkins, H. S., Butt, L. E., Cox, P. A., Gowers, D. M., Vincent, H. A., & Callaghan, A. J. (2020). Identification and analysis of novel small molecule inhibitors of RNase E: Implications for antibacterial targeting and regulation of RNase E. *Biochemistry and Biophysics Reports*, *23*, 1–9.

Mauger, D. M., Joseph Cabral, B., Presnyak, V., Su, S. V., Reid, D. W., Goodman, B., Link, K., Khatwani, N., Reynders, J., Moore, M. J., & McFadyen, I. J. (2019). mRNA structure regulates protein expression through changes in functional half-life. *Proceedings of the National Academy of Sciences*, *116*, 24075–24083.

McElwain, L., Phair, K., Kealey, C., & Brady, D. (2022). Current trends in biopharmaceuticals production in *Escherichia coli*. *Biotechnology Letters*, *44*, 917–931.

Miroux, B., & Walker, J. E. (1996). Over-production of proteins in *Escherichia coli*: Mutant hosts that allow synthesis of some membrane proteins and globular proteins at high levels. *Journal of Molecular Biology*, *260*, 289–298.

Mohanty, B. K., & Kushner, S. R. (2019). New insights into the relationship between tRNA processing and polyadenylation in *Escherichia coli*. *Trends in Genetics*, *35*, 434–445.

Mohanty, B. K., & Kushner, S. R. (2022). Regulation of mRNA decay in *E. coli*. *Critical Reviews in Biochemistry and Molecular Biology*, *57*, 48–72.

Nelissen, F. H. T., Leunissen, E. H. P., Van De Laar, L., Tessari, M., Heus, H. A., & Wijmenga, S. S. (2012). Fast production of homogeneous recombinant RNA-towards large-scale production of RNA. *Nucleic Acids Research*, *40*, e102.

Nwokeoji, A. O., Kilby, P. M., Portwood, D. E., & Dickman, M. J. (2016). RNASwift: A rapid, versatile RNA extraction method free from phenol and chloroform. *Analytical Biochemistry*, *512*, 36–46.

Ouranidis, A., Vavilis, T., Mandala, E., Davidopoulou, C., Stamoula, E., Markopoulou, C. K., Karagianni, A., & Kachrimanis, K. (2022). mRNA therapeutic modalities design, formulation and Manufacturing under pharma 4.0 principles. *Biomedicines*, *10*, 50.

Pertzev, A. V. (2006). Characterization of RNA sequence determinants and antideterminants of processing reactivity for a minimal substrate of *Escherichia coli* ribonuclease III. *Nucleic Acids Research*, *34*, 3708–3721.

Plank, T. D. M., Whitehurst, J. T., & Kieft, J. S. (2013). Cell type specificity and structural determinants of IRES activity from the 5′ leaders of different HIV-1 transcripts. *Nucleic Acids Research*, *41*, 6698–6714.

Ponchon, L., Beauvais, G., Nonin-Lecomte, S., & Dardel, F. (2009). A generic protocol for the expression and purification of recombinant

RNA in *Escherichia coli* using a tRNA scaffold. *Nature Protocols*, *4*, 947–959.

Ponchon, L., Catala, M., Seijo, B., El Khouri, M., Dardel, F., Nonin-Lecomte, S., & Tisné, C. (2013). Co-expression of RNA-protein complexes in *Escherichia coli* and applications to RNA biology. *Nucleic Acids Research*, *41*, e150.

Ponchon, L., & Dardel, F. (2011). Large scale expression and purification of recombinant RNA in *Escherichia coli*. *Methods*, *54*, 267–273.

Pontrelli, S., Chiu, T. Y., Lan, E. I., Chen, F. Y. H., Chang, P., & Liao, J. C. (2018). *Escherichia coli* as a host for metabolic engineering. *Metabolic Engineering*, *50*, 16–46.

Prossliner, T., Agrawal, S., Heidemann, D. F., Sørensen, M. A., & Svenningsen, S. L. (2023). tRNAs are stable after all: Pitfalls in quantification of tRNA from starved *Escherichia coli* cultures exposed by validation of RNA purification methods. *mBio*, *14*, 1–18.

Qin, C., Xiang, Y., Liu, J., Zhang, R., Liu, Z., Li, T., Sun, Z., Ouyang, X., Zong, Y., Zhang, H. M., Ouyang, Q., Qian, L., & Lou, C. (2023). Precise programming of multigene expression stoichiometry in mammalian cells by a modular and programmable transcriptional system. *Nature Communications*, *14*(1), 1500.

Qin, S., Tang, X., Chen, Y., Chen, K., Fan, N., Xiao, W., Zheng, Q., Li, G., Teng, Y., Wu, M., & Song, X. (2022). mRNA-based therapeutics: Powerful and versatile tools to combat diseases. *Signal Transduction and Targeted Therapy*, *7*, 166.

Qu, L., Yi, Z., Shen, Y., Lin, L., Chen, F., Xu, Y., Wu, Z., Tang, H., Zhang, X., Tian, F., Wang, C., Xiao, X., Dong, X., Guo, L., Lu, S., Yang, C., Tang, C., Yang, Y., Yu, W., … Wei, W. (2022). Circular RNA vaccines against SARS-CoV-2 and emerging variants. *Cell*, *185*, 1728–1744.

Radoš, D., Donati, S., Lempp, M., Rapp, J., & Link, H. (2022). Homeostasis of the biosynthetic *E. coli* metabolome. *IScience*, *25*, 104503.

Richards, J., & Belasco, J. G. (2016). Distinct requirements for 5′-monophosphate-assisted RNA cleavage by *Escherichia coli* RNase E and RNase G. *Journal of Biological Chemistry*, *291*, 5038–5048.

Richards, J., & Belasco, J. G. (2023). Graded impact of obstacle size on scanning by RNase E. *Nucleic Acids Research*, *51*, 1364–1374.

Rosa, S. S., Prazeres, D. M. F., Azevedo, A. M., & Marques, M. P. C. (2021). mRNA vaccines manufacturing: Challenges and bottlenecks. *Vaccine*, *39*, 2190–2200.

Rostain, W., Shen, S., Cordero, T., Rodrigo, G., & Jaramillo, A. (2020). Engineering a circular riboregulator in *Escherichia coli*. *BioDesign Research*, *2020*, 1–9.

Rouches, M. V., Xu, Y., Cortes, L. B. G., & Lambert, G. (2022). A plasmid system with tunable copy number. *Nature Communications*, *13*, 3908.

Roux, C., Etienne, T. A., Hajnsdorf, E., Ropers, D., Carpousis, A. J., Cocaign-Bousquet, M., & Girbal, L. (2022). The essential role of mRNA degradation in understanding and engineering *E. coli* metabolism. *Biotechnology Advances*, *54*, 107805.

Sandomenico, A., Sivaccumar, J. P., & Ruvo, M. (2020). Evolution of *Escherichia coli* expression system in producing antibody recombinant fragments. *International Journal of Molecular Sciences*, *21*, 6324.

Scheel, R. A., Ho, T., Kageyama, Y., Masisak, J., McKenney, S., Lundgren, B. R., & Nomura, C. T. (2021). Optimizing a fed-batch high-density fermentation process for medium chain-length poly(3-hydroxyalkanoates) in *Escherichia coli*. *Frontiers in Bioengineering and Biotechnology*, *9*, 1–16.

Soini, J., Ukkonen, K., & Neubauer, P. (2008). High cell density media for *Escherichia coli* are generally designed for aerobic cultivations—Consequences for large-scale bioprocesses and shake flask cultures. *Microbial Cell Factories*, *7*, 26.

Soto, R., Caspeta, L., Barrón, B., Gosset, G., Ramírez, O. T., & Lara, A. R. (2011). High cell-density cultivation in batch mode for plasmid DNA production by a metabolically engineered *E. coli* strain with minimized overflow metabolism. *Biochemical Engineering Journal*, *56*, 165–171.

Sripada, S. A., Chu, W., Williams, T. I., Teten, M. A., Mosley, B. J., Carbonell, R. G., Lenhoff, A. M., Cramer, S. M., Bill, J., Yigzaw, Y., Roush, D. J., & Menegatti, S. (2022). Towards continuous mAb purification: Clearance of host cell proteins from CHO cell culture harvests via "flow-through affinity chromatography" using peptide-based adsorbents. *Biotechnology and Bioengineering*, *119*, 1873–1889.

Studier, F. W., & Moffatt, B. A. (1986). Use of bacteriophage T7 RNA polymerase to direct selective high-level expression of cloned genes. *Journal of Molecular Biology*, *189*, 113–130.

Vavilis, T., Stamoula, E., Ainatzoglou, A., Sachinidis, A., Lamprinou, M., Dardalas, I., & Vizirianakis, I. S. (2023). mRNA in the context of protein replacement therapy. *Pharmaceutics*, *15*, 166.

Viegas, S. C., Apura, P., Martínez-García, E., De Lorenzo, V., & Arraiano, C. M. (2018). Modulating heterologous gene expression with portable mRNA-stabilizing 5′-UTR sequences. *ACS Synthetic Biology*, *7*, 2177–2188.

Wesselhoeft, R. A., Kowalski, P. S., & Anderson, D. G. (2018). Engineering circular RNA for potent and stable translation in eukaryotic cells. *Nature Communications*, *9*, 2629.

Whitley, J., Zwolinski, C., Denis, C., Maughan, M., Hayles, L., Clarke, D., Snare, M., Liao, H., Chiou, S., Marmura, T., Zoeller, H., Hudson, B., Peart, J., Johnson, M., Karlsson, A., Wang, Y., Nagle, C., Harris, C., Tonkin, D., … Johnson, M. R. (2022). Development of mRNA manufacturing for vaccines and therapeutics: mRNA platform requirements and development of a scalable production process to support early phase clinical trials. *Translational Research*, *242*, 38–55.

Williams, D. J., Puhl, H. L., & Ikeda, S. R. (2010). A simple, highly efficient method for heterologous expression in mammalian primary neurons using cationic lipid-mediated mRNA transfection. *Frontiers in Neuroscience*, *4*, 1–20.

Yang, D., Prabowo, C. P. S., Eun, H., Park, S. Y., Cho, I. J., Jiao, S., & Lee, S. Y. (2021). *Escherichia coli* as a platform microbial host for systems metabolic engineering. *Essays in Biochemistry*, *65*, 225–246.

Youssef, M., Hitti, C., Puppin Chaves Fulber, J., & Kamen, A. A. (2023). Enabling mRNA therapeutics: Current landscape and challenges in manufacturing. *Biomolecules*, *13*, 1497.

Zhang, H., Zhang, L., Lin, A., Xu, C., Li, Z., Liu, K., Liu, B., Ma, X., Zhao, F., Jiang, H., Chen, C., Shen, H., Li, H., Mathews, D. H., Zhang, Y., & Huang, L. (2023). Algorithm for optimized mRNA design improves stability and immunogenicity. *Nature*, *621*, 396–403.

Zhang, Q., Ma, D., Wu, F., Standage-Beier, K., Chen, X., Wu, K., Green, A. A., & Wang, X. (2021). Predictable control of RNA lifetime using engineered degradation-tuning RNAs. *Nature Chemical Biology*, *17*, 828–836.

Ziegler, M., Zieringer, J., Döring, C. L., Paul, L., Schaal, C., & Takors, R. (2021). Engineering of a robust *Escherichia coli* chassis and exploitation for large-scale production processes. *Metabolic Engineering*, *67*, 75–87.

SUPPORTING INFORMATION

Additional supporting information can be found online in the Supporting Information section at the end of this article.

How to cite this article: Curry, E., Muir, G., Qu, J., Kis, Z., Hulley, M., & Brown, A. (2024). Engineering an *Escherichia coli* based in vivo mRNA manufacturing platform. *Biotechnology and Bioengineering*, 1–15. https://doi.org/10.1002/bit.28684